Lowland Technology International 2018; 20 (3): 245-258
International Association of Lowland Technology (IALT): ISSN 1344-9656

Research Paper

Field validated prediction of latent slope failure based on cracked soil approach

S. Alexsander [1], I.B. Mochtar [2] and W. Utama [3]

ARTICLE INFORMATION

Article history:

Received: 15 November, 2017
Received in revised form: 12 August, 2018
Accepted: 12 September, 2018
Publish on: 07 December, 2018

Keywords:

Cracks soil
Induced polarization
Land sliding
Slope stability
Tomography resistivity

ABSTRACT

This study is to prove the existence of latent sliding of a suspected unstable slope using the cracked soils approach. This study was initiated by trying to map the cracks inside soil slope by means of measuring the Tomographic Resistivity, TR, and Induced Polarization, IP, of the soil at the slope prior to performing stability analysis of the slope. To map the cracks inside the slope at the study location, 3 lines of TR and IP were performed. The results of the 3-line mapping showed the existence of sliding plane toward the slope edge at a depth between 3 – 5 meters below the soil surface, and the sliding plane was about 30 – 50 meters in length. With the cracks and possible sliding planes were known, the cracks could be drawn in 3-dimentional model, as part of the topographical map of the slope. This study had predicted that another slope sliding would occur at the area where the highest stresses and strains concentration were located. It was at this location exactly that another slope sliding had occurred several months afterwards when heavy rain came.

1. Introduction

In Indonesia specially on Java, Central and South Sumatra, Borneo Island and South Celebes, rain falls in 2016 had been recorded to increase 2.8 times the normal condition. During period 2016 the soil sliding and slope failure had occurred at 464 locations in all throughout Indonesia (much higher than normal), and most of the slope failures occurred during the maximum rainfall between December 2016 to March 2017 (Indonesia Food Security Monitoring, 2016). Therefore, there seemed to be a definite correlation between the high rain falls and slope failures.

On December 2th, 2016, slope failure had occurred in the village of Sumberjo, District Selorejo, Blitar, Indonesia, as it seen in **Fig. 1** (Alexander et. al., 2017). Based on rain measurement, the rain had fallen for about 10 hours before the slope failure with total rainfall intensity of 102 mm in 10 hours. The rain at the location of study during the 10 hours period of observation had fallen as combination of light rain, heavy rain to very heavy rain. Since the above slope had been stable for many years before under many rains, the apparent question would be whether the duration of rain or the intensity of rain that caused the slope failure.

The cracked soil approach developed by Mochtar (2012) has been able to answer that high intensity rain and the already existence of deep cracks inside soil are both as the main factors in determining the stability of slopes. Furthermore, Alexander et. al. (2017) has been

[1] Phd Student of Civil Engineering, Institut Teknologi Sepuluh Nopember, Surabaya, INDONESIA, stephanusalexsander@gmail.com
[2] Professor of Civil Engineering, Institut Teknologi Sepuluh Nopember, Surabaya, INDONESIA, indramochtar.mochtar@gmail.com
[3] Lecturer of Geophysic Engineering, Institut Teknologi Sepuluh Nopember, Surabaya, INDONESIA, wu.explorer@gmail.com
Note: Discussion on this paper is open until June 2019

able to develop the above method by introducing a method of estimating the possible place and extend of the cracks inside soil.

In this paper, the method of Alexsander above is further tried on slope failure evidence at the Village of Sumberejo, Blitar, Indonesia. It is found that the method of Alexander can also be used to predict latent slope failure that may occur in the future, which is proven afterwards.

The study in this paper used crack soil approach to predict the position of failure inside the slope that would have occurred after the next heavy rainfall. The cracks soil approach in this study is the first attempt by the writers to map the cracks inside the soil in 3-dimension model. When rain entered into the cracks, the soil part containing many cracks would have become saturated immediately, so that the pore water pressure would have significantly increased inside the crack. To map the cracks inside the slope, the tomographic resistivity (TR) and Induced Polarization (IP) measurement were used. Afterward, analysis of slope stability was applied using Geotechnical Engineering approach with the help of "Midas GTS NX software" so that, the deformation of the slope, maximum stresses inside the slope, water pressure along the cracks and the final Safety Factor of the slope could be estimated.

Fig. 1. Slope failure occurred in Sumberjo Village, Blitar Indonesia (Alexander, 2017).

2. Backgroud of Cracked Soil Aprroach to Slope Failure

Many researchers had investigated the effect of rain to landslide. The researchers on unsaturated soils correlated the rain with the change in suction matrix and negative water pressure. Rain water would infiltrate into the soil and reduce the suction matrix of the soil (Fredlund and Raharjo, 1993; Griffith and Lu, 2005). Furthermore, the rain water infiltration could also cause gradual reduction of the suction matrix in the unsaturated soil (Regmi et. al. 2011). Generally, with the existence of water intrusion into soil, the pore water pressure in the soil would have increased and the effective soil stresses would have decreased, to be followed by the decrease of soil strength. However, the above researches could not explain why slope failures mostly occurred due to heavy to very heavy rains and almost never due to low to moderate rains, since any type of rain could cause reduction of soil suction matrix.

Some other researchers had also conducted studies on the existence of relatively shallow tension cracks in soils surface such as Wang,Y et. al. (2013), and Sánchez, M et.al. (2014). These researchers showed and modelled the cracks that existed on slope surfaces. However, the existence of shallow cracks along the soil surface could not be made to explain how the deep slope failures could have occurred, as they were mostly in reality.

Infiltration of rain water into the soil was very much related to the soil permeability. At the Sumberjo Village location, the soil was silty sand with the soil permeability could be estimated between 10^{-4} to 10^{-2} mm/sec (Das,

2008). In Soil Mechanics the velocity of water infiltration into soil could be assumed to follow the Darcy's formula:

$$V = k.\ i. \quad [1]$$

where:
V = velocity of water infiltration into soil (mm/sec)
k = permeability coefficient (mm/sec),
i = hydraulic gradient.

If in this case it was assumed that the hydraulic gradient, i = 1, and also assuming the soil permeability value was 10^{-2} mm/sec, the amount of water infiltration into the soil was merely about 360 mm (= 0.36 m) for 10 hours duration of continuous rain (the penetration would be much smaller if the soil permeability values were merely 10^{-4} mm/sec). This meant that the 10 hours heavy rain should only cause water penetration into the soil to a maximum depth of 0.36 m, which was certainly not enough to cause deep landslide as it was in reality.

Furthermore, at the area chosen for this study in Sumberjo Village, rain had fallen for many years repeatedly and the heaviest rain might have penetrated the soil to maximum of 0.36 m only. Without the existence of deeper cracks, the rain water could not penetrate deep into the soil to have caused slope failure.

If cracks did not have prevailed inside the slope and if rain was the only cause of slope failure, slope failure would have occurred in large area around the village, and not to be confined in a particular location only. This was because the village was surrounded by slopes of almost the same soil types, the same slope inclination, the same vegetation covering the slopes, and subjected under the same intensity of rain. Therefore, slope failure should have occurred throughout the whole village. Yet, in reality the slope failure occurred at one particular location only. Most of the slopes around the village were still intact.

Several experts like Duncan et al (2000) and Tang et al (1999) so far had tried to solve slope stability problem based on back calculation method, by reducing the soil shear strength of the value ϕ and cohesion c, much lower than the actual measured values from laboratory investigation so that the calculated Safety Factor of the slope became 1.0 (slope critical condition). The selected ϕ and c were of those to cause the Safety Factor ≤ 1. This method actually did not correlate with the actual soil condition, because the effect of rain in theory did not change any ϕ and c value of the soil. Furthermore, the method was not also able to explain why failure occurred at the particular location of slope only. If the rain was causing reduction of soil strength parameters as expected, the whole slope along mountainous region would have slided simultaneously under heavy or very heavy rainfall; yet in reality the slope failure always occurred at certain particular slope only.

Up to recently, many experts believed that rain would have caused the slope to become saturated first; but this condition contradicted the reality shown by Mochtar (2012), who stated that only few slope failures showed the sign of small water flow coming out from the soil. The slope failure in general showed almost dry soil slope, or partially moist soils, on the remaining slope. Therefore as shown in **Fig. 2**, taken just after failure, the typical remain of slope failures in general is that the soil layers are slightly moist only near the top, but mostly dry at other parts of the soil layers at the failure slopes.

Fig. 2. Typical mostly dry and moist soil layers along the failured slope (assumption of saturated slope prior to failure is not proven). (Source: Alexander, 2017).

It has been shown by slope failure phenomena above, which during failure only certain part of the slope indicating an intrusion of water, there should be good explanation why failure occurred at particular location only and why rain water had not effect the whole length of the slope. The explanation about this partial failure of slope may be given when the assumption is based on cracked soil phenomena. The cracked soil approach in this paper was used by the writers to prove the mechanism of sliding on a 9 m height embankment fill behind a retaining wall. It had been proven by the writers in other publication (Alexsander et al, 2017) that the failure followed exactly the pattern of cracks inside the soil, and it was also due to the existence of water pressure built up inside the cracks during heavy rain.

The hypothesis of cracked soil was first introduced by Mochtar (2012) after making many observation about slope failures after heavy rainfall. The main factors of causing the failure according to Mochtar (2012) were the existence of many cracks inside slope and propagation of the cracks. During heavy rain, the cracks were filled up to the top with water that had caused tremendous water pressure inside the cracks so that the slope might fail. However, propagation of cracks inside the slope were different from one slope to the other, the slope with more advanced cracks would have slide first. Sliding would occur only when the crack propagation was similar to that of the sliding pattern. Otherwise, the slope with different pattern of cracks may not fail at all. This was the explanation why only the slope at a particular location underwent failure, not all the slopes along the same stretch of hill slopes simultaneously, during heavy rain.

3. Mapping of the location and geological condition of the study area

The study was conducted at the Sumberjo Village, the area was with coordinate 65869; 910059 UTM until 65811; 9100536 UTM. The result of mapping are given in **Fig. 3**, while the geological condition can be seen at **Fig. 4**.

The geological condition of the study area was known from the regional geological map of Blitar (Obtained by Sjarifuddin et al, 1992), which is shown in **Fig. 4**. Location of study also appear as Wuni formation and Mount Butak sediment. Thickness of the Mount of Mount Butak sediment above the Wuni formation is about 2000 m. The Mount Butak sediments consist of lava, vulcanic breccia, tuff breccia and sandy tuff.

The soils formed at the location of this study comprise of mostly sedimentation from Mount Butak eruption, so that nonuniformity of the soil formation should be very likely. The nonuniformity of the soil formation can also be detected from the existence sandy tuff. This sandy tuff has specific-gravity lower than normal sandy soil. Based on testing on some sandy tuff from other part at of Kalimantan and Java. The Specific Gravity of this sandy tuff material is < 2.4 (according to PT. Cemara Geo Engineering, 2012 – 2014) which is much lower than normal sandy soil in general (Specific Gravity 2.6 – 2.75). Specific Gravity lower than normal could affect to stability of slope in heavy rainfall where the run off could easily carry sand particles

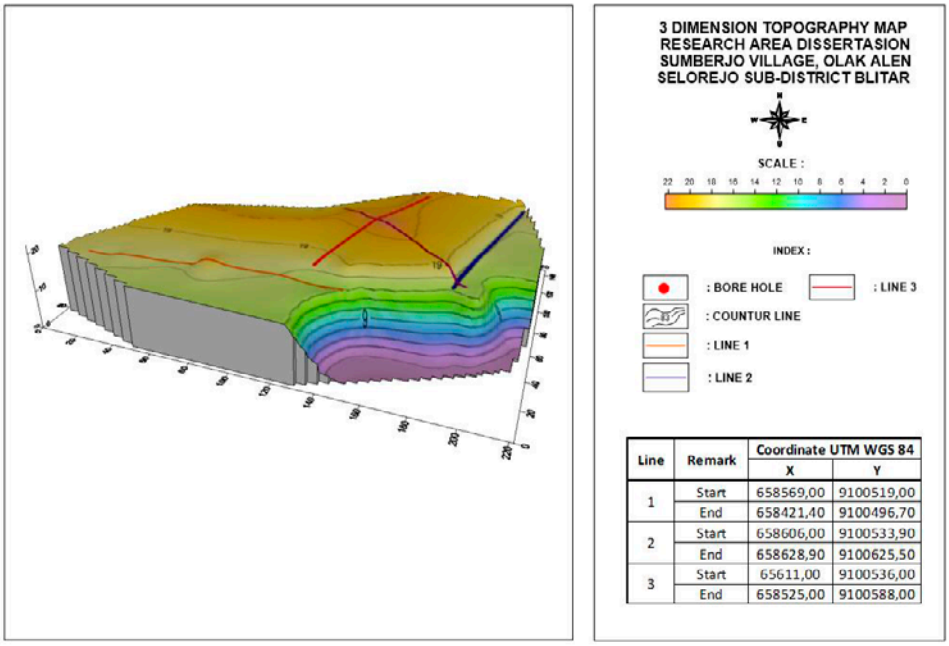

Line	Remark	Coordinate UTM WGS 84	
		X	Y
1	Start	658569,00	9100519,00
	End	658421,40	9100496,70
2	Start	658606,00	9100533,90
	End	658628,90	9100625,50
3	Start	65611,00	9100536,00
	End	658525,00	9100588,00

Fig. 3. Area and shape of the study location and geoelectric survey lines.

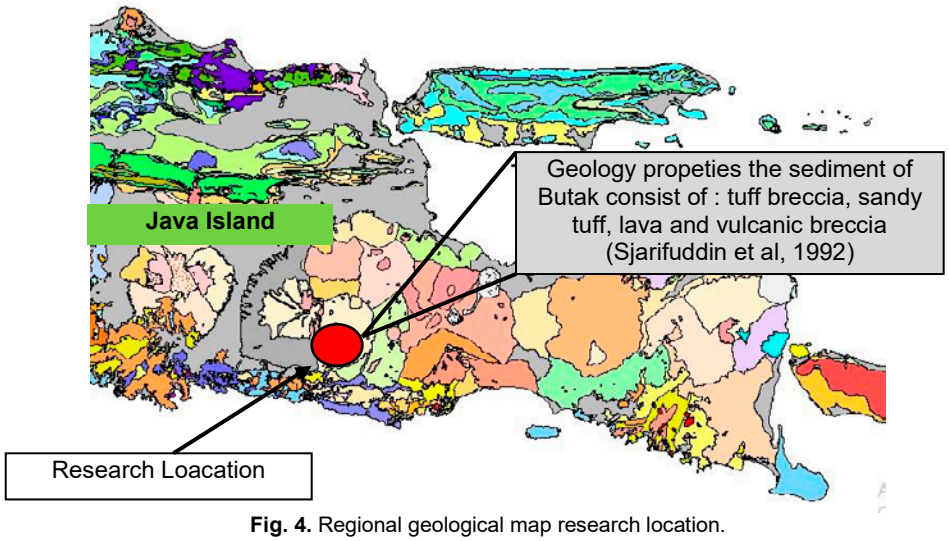

Fig. 4. Regional geological map research location.

4. Result of tomographic resistivity, TR and induced polarization, IP interpretation at the laboratory and location of study

During this study, 3 lines of geoelectric mapping were performed to detect existence of cracks and slope failure plane at the study location. The result of geoelectric can be seen in **Figs. 5 to 7**.

The magnitude of TR value along the failure plane are 18.58 – 78.93 ohm.m and these values appears along 50 to 55 meters length of the slope with direction of the cracks similar to the direction of slope failure. Furthermore, just below failure plane one could locate the cracks from the IP values that range between 0.72 – 15.40 %, occurring in Line 1. For Line 2 the failure plane is shown with TR values between 12.99 – 18.83 ohm.m to spread for 40 – 42 meters length with IP value of 0.52 – 39.31 %. For Line 3 the failure plane shown TR value 15.44 – 23.47 ohm.m which is spreading for 30 – 36 meters with IP value of 2.61 – 45.56 %.

To determine the cracks existed inside the slope by means of reading the IP results, the following interpretations are suggested:

1. High IP results represent the possibility of cracks inside the soil. Then, one may draw the possible cracks, especially of those similar with the sliding failure pattern of the slope.
2. From the results of Tomographic Resistivity values, the possible sliding plane should be along the areas with higher water contents, which is also along the areas with very low reading of TR.

By adjusting and trying several times from some alternative possible sliding planes, and then by calculating from every possible sliding plane the value of the slope safety factor, SF, one could determine the actual sliding plane that would have occurred in the field.

From this analysis, 3 patterns of the cracks were formed. The 3 patterns of cracks would be modelled into 3-dimension numerical model. However, when the first shallower crack where modelled in 3-dimension analysis with the help of Midas GTS NX program, it was apparent that is shallow cracks analysis had yield safety factor of the slope < 1. This shallower crack has predicted the actual place where the next sliding would have occurred when heavy rainfall came, and this prediction was later proven exactly with sliding of the part of the slope exactly at prediction area, several months after is has studied.

5. Result of soil investigation as input material properties for software Midas GTS NX

5.1 Result of Field and Laboratory Soil Investigation

Soil investigation was performed using SPT and boring test to obtain soil samples. From boring test to the depth of 30 meter at the study location, six layers of soil were obtained and they were predominantly of soil from loose silty sand to very dense silty sand, soil such as those given **Fig. 8**. For laboratory test result, the soil parameters are given in **Table 1**.

5.2 Geotechnical Parameters to be used as input Parameters into the Software Midas GTS NX

In this study, the selected constitutive model for soil is the Modified Mohr Coulomb model included Hardening Soil, so that the model called Modified Mohr Coulomb with hardening (MMC-hardening). The choice of this model was determined from case study examples given

the in the software Midas GTS NX (release note Midas GTS NX, 2014), where the cases of soil models were compared, which where: Mohr Coulomb, Modified Mohr Coulumb and Modified Mohr Coulomb Model with soil hardening. From the three soil models the MMC-hardening model showed the most representative and detail reponse. The soil models parameters to be used can be seen in **Fig. 9**. In **Fig. 9**, the sequence of selected parameters are shown in details to be in analysis with MMC - hardening soil model The results of SPT test were then utilized to model the soil layers in situ when slope stability analysis was performed. The result of laboratory soil test were also used, especially when inputting soil material properties for the software Midas GTS NX. For the Young Modulus (E_U) parameter of the soil, the equations developed by Web (1969), as given in Equation 2 and 3 were adopted. The Young Modulus equation were applied for the loose to medium and dense soil

Furthermore, there were other soil parameters used as input to the software, they were : soil density (γ), E_{50}^{ref} (stiffness modulus at 50 % strength at certain reference in triaxial test with confining pressure 100 KPa), E_{oed} (tangensial modulus), E_{ur} (stiffness modulus for unloading and reloading), C (cohesion), ϕ' (angles of internal friction), ψ' (angle of dilatancy. The whole parameters used in the equation can be seen in **Table 2**.

$E_u = 500\ (N_{55} + 15)$ (for loose to medium soil) [2]

$E_u = 18000 + (750\ x\ N_{55})$ (for dense soil) [3]

where

E_u = modulus young (Kn/m^2)

N_{55} = SPT N value corrected to 55% of the theoretical free fall hammer energy

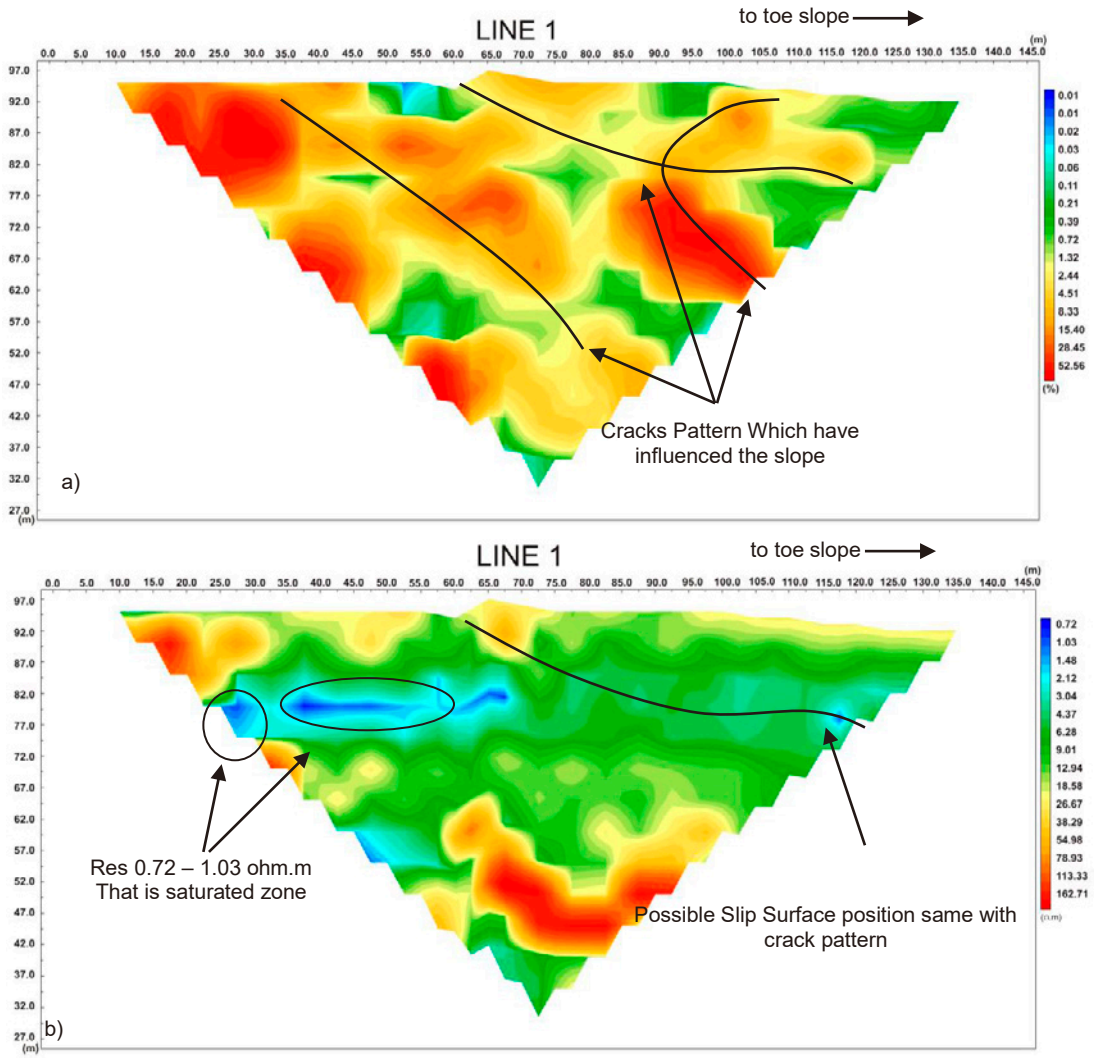

Fig 5. Interpretation result of Line 1, showing the existence of cracks pattern that might have influenced the slope stability. (a). Result of Induced Polarization, (b). Result of Tomography Resistivity.

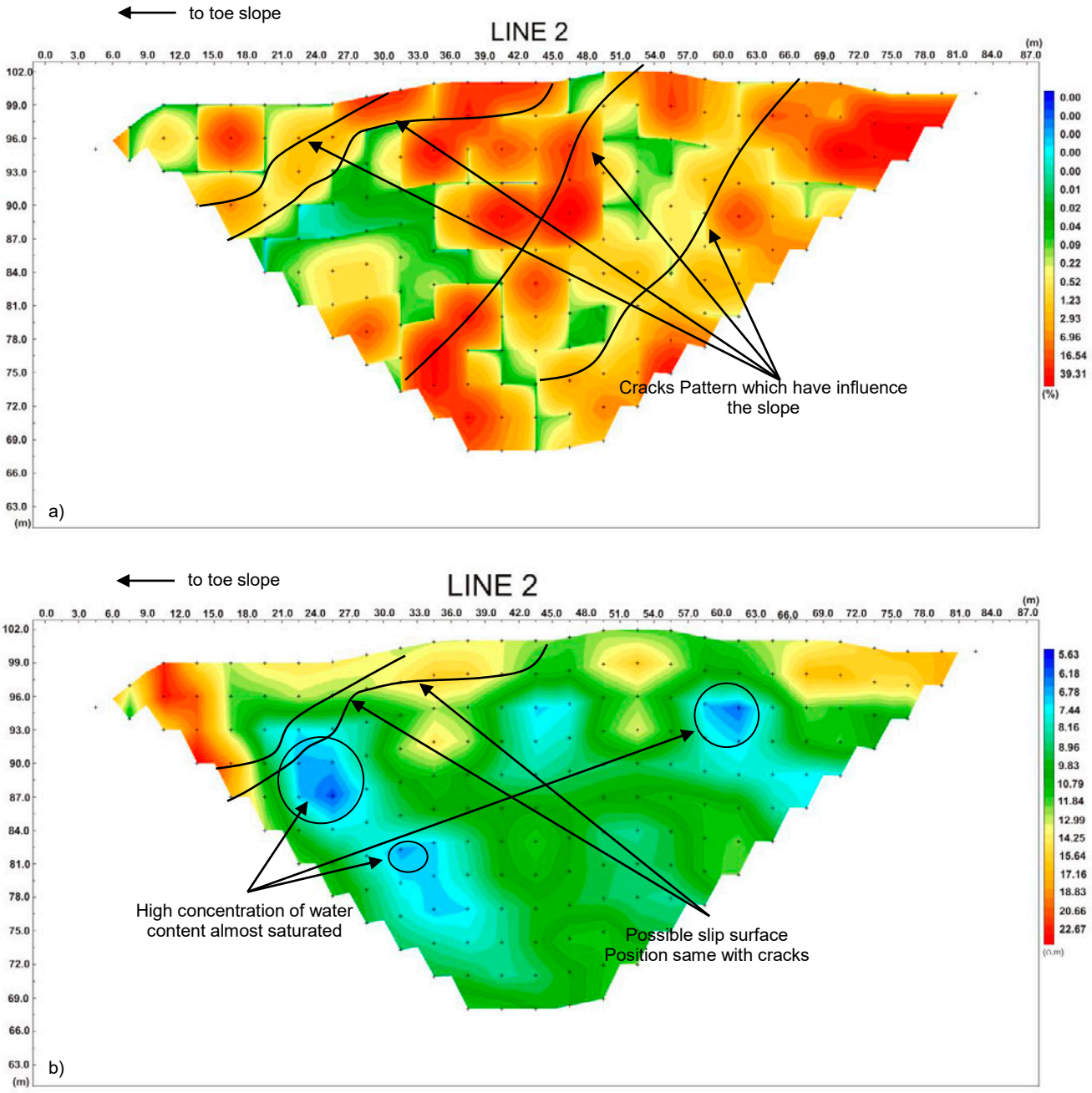

Fig. 6. Interpretation result of Line 2, showing the existence of cracks pattern that influence the slope stability. (a). Result of Induced Polarization, (b). Result of Tomography Resistivity.

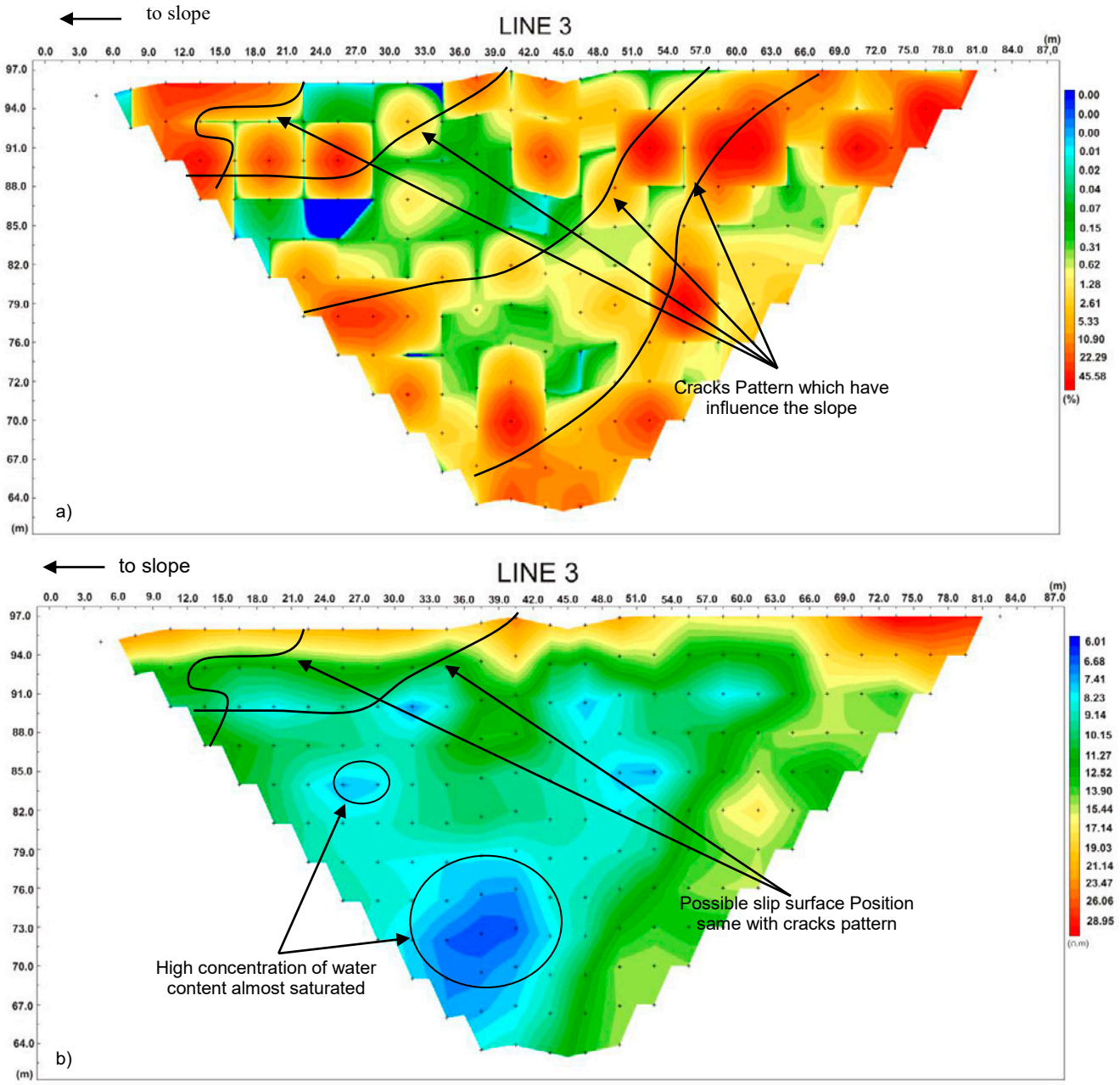

Fig. 7. Interpretation result of Line 3, showing the existence of cracks pattern that influenced the slope stability. (a). Result of Induced Polarization, (b). Result of Tomography Resistivity.

DRILLING LOG

Drilling Location : Sumberejo Distrrict, Olak Alen Village - Blitar
Project Name : Landslide Research
Company : Thesis - Research

Elevation : - m
Total Length of Drill : 30 m
Drill Machine : Spindel
Bor Master : Serilus Bani
Analysis By : Rety Winonazada
Check analysis By : Joko Aprianto, ST
STANDART PENETRATION TEST (SPT TEST)

Scale	Depth (m)	Thikness (m)	GWL	Symbol	Description	Consistensy	Core Recovery (%)	SOIL CLASSIFICATION	Method Sample UDS & SPT	Thikness (m)	Depth (m)	Blows Penetration Each 15cm 15 cm	15 cm	15 cm	N Blows N2+N3 30cm
-0,5											-0,5				
-1,0											-1,0				
-1,5		2,00			Silty Sand			SP-SM		0,50	-1,5				
-2,0	2,0					Loose				0,45	-2,0	2	3	3	6
-2,5											-2,5				
-3,0											-3,0				
-3,5		2,00			Silty Sand			SP-SM		0,50	-3,5				
-4,0	4,0					Loose				0,45	-4,0	4	4	5	9
-4,5											-4,5				
-5,0											-5,0				
-5,5		2,00			Silty Sand			SP-SM		0,50	-5,5				
-6,0	6,0					Medium Dense				0,45	-6,0	5	5	7	12
-6,5											-6,5				
-7,0											-7,0				
-7,5		2,00			Silty Sand			SP-SM		0,50	-7,5				
-8,0	8,0					Medium Dense				0,45	-8,0	5	5	7	12
-8,5											-8,5				
-9,0											-9,0				
-9,5		2,00			Silty Sand			SP-SM		0,50	-9,5				
-10,0	10,0					Medium Dense				0,45	-10,0	6	6	7	13
-10,5											-10,5				
-11,0											-11,0				
-11,5		2,00			Silty Sand			SP-SM		0,50	-11,5				
-12,0	12,0					Medium Dense				0,45	-12,0	7	8	8	16
-12,5											-12,5				
-13,0											-13,0				
-13,5		2,00			Silty Sand			SP-SM		0,50	-13,5				
-14,0	14,0					Dense				0,45	-14,0	10	11	13	24
-14,5											-14,5				
-15,0											-15,0				
-15,5		2,00			Silty Sand			SP-SM		0,50	-15,5				
-16,0	16,0					Dense				0,45	-16,0	10	14	16	30
-16,5											-16,5				
-17,0											-17,0				
-17,5		2,00			Silty Sand			SP-SM		0,50	-17,5				
-18,0	18,0					Very Dense				0,45	-18,0	10	14	19	33
-18,5											-18,5				
-19,0											-19,0				
-19,5		2,00			Silty Sand			SP-SM		0,50	-19,5				
-20,0	20,0					Very Dense				0,45	-20,0	12	17	23	40
-20,5											-20,5				
-21,0											-21,0				
-21,5		2,00			Silty Sand			SP-SM		0,50	-21,5				
-22,0	22,0					Dense				0,45	-22,0	10	14	16	30
-22,5											-22,5				
-23,0											-23,0				
-23,5		2,00			Silty Sand			SP-SM		0,50	-23,5				
-24,0	24,0					Very Dense				0,45	-24,0	14	19	24	43
-24,5											-24,5				
-25,0											-25,0				
-25,5		2,00			Silty Sand			SP-SM		0,50	-25,5				
-26,0	26,0					Very Dense				0,45	-26,0	14	21	26	47
-26,5											-26,5				
-27,0											-27,0				
-27,5		2,00			Silty Sand			SP-SM		0,50	-27,5				
-28,0	28,0					Very Dense				0,45	-28,0	16	23	28	51
-28,5											-28,5				
-29,0											-29,0				
-29,5		2,00			Silty Sand			SP-SM		0,50	-29,5				
-30,0	30,0					Very Dense	BOR STOP			0,45	-30,0	18	24	28	52

N Value Graph: 0 20 40 60

LEGENDS SYMBOLS AND RANGE OF VALUE

LEGEND :

- Standard Penetration Test (SPT)
- Undisturbed Sample (US)
- Disturbed Sample (DS)
- Ground Water Level (GWL)

SOIL CLASSIFICATION SYMBOL

GRAVEL	: G
SAND	: S
SILT	: M
CLAY	: C
ORGANIC	: O
WELL	; W
POOR	; P
HIGH	; H
LOW	; L

COHESIVE SOIL

CONSISTENSY		N VALUE
VERY SOFT	:	0 - 1
SOFT	:	2 - 4
MEDIUM SOFT	:	5 - 8
STIFF	:	9 - 15
VERY STIFF	:	16 - 30
HARD	:	31 - 60
VERY HARD	:	> 60

GRANULAR SOIL

DENSITY	N - VALUE
VERY LOOSE	: 0 - 4
LOOSE	: 5 - 10
EDIUM DENSE	: 11 - 24
DENSE	: 25 - 50
VERY DENSE	: > 50

ROCK QUALITY DESIGNATION (RQD)

DESCRIPTION	R 20 %
VERY POOR	< 25
POOR	25 - 50
FAIR	51 -75
GOOD	76 - 90
EXCELLENT	> 90

Fig. 8. The result of soil Investigation for SPT and Boring.

Table 1. Laboratory Test Result on Soil Samples obtain from boring test.

Depth (meter)	Soil Description	USCS	Unit weight		*Spesific Gravity*	Liquid Limit (%)	Plastisity of index (%)	*Direct Shear*	
			γ_{moist} (gr/cm^3)	γ_{dry} (gr/cm^3)				φ (°)	C kg/cm^2
1.50	Silty Sand	SP-SM	1.40	0.98	2.268	51.83	10.72	29.17	0.14
3.50	Silty Sand	SP - SM	1.48	0.99	2.359	51.51	9.44	28.87	0.14
5.50	Silty Sand	SP - SM	1.14	0.71	1.898	-	-	28.27	0.13
7.50	Silty Sand	SP - SM	1.28	0.72	2.273	-	-	28.57	0.13
9.50	Silty Sand	SP - SM	1.16	0.67	2.223	61.67	12.35	29.46	0.12
11.50	Silty Sand	SP - SM	1.32	0.82	2.160	60.01	16.96	29.76	0.13
13.50	Silty Sand	SP - SM	1.17	0.67	2.058	-	-	30.63	0.12
15.50	Silty Sand	SP - SM	1.50	1.00	2.370	60.22	11.54	30.34	0.14
17.50	Silty Sand	SP - SM	1.41	0.83	2.037	66.30	14.27	30.92	0.12
19.50	Silty Sand	SP - SM	1.41	0.95	2.188	64.04	14.75	31.77	0.12
21.50	Silty Sand	SP - SM	1.35	0.81	2.558	56.23	18.96	30.05	0.12
23.50	Silty Sand	SP - SM	1.55	0.95	2.393	56.72	23.52	31.49	0.16
25.50	Silty Sand	SP - SM	1.41	0.81	2.460	55.27	13.20	32.61	0.13
27.50	Silty Sand	SP - SM	1.70	1.11	2.393	54.73	16.24	33.43	0.14
29.50	Silty Sand	SP - SM	1.45	0.93	2.290	98.64	50.07	33.70	0.12

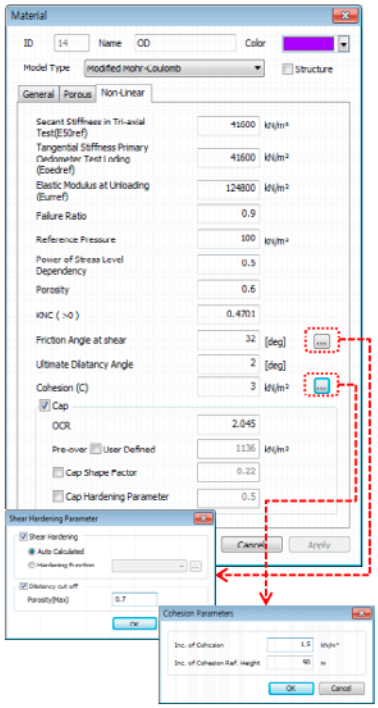

Parameter	Description	Reference value (kN, m)
	Soil stiffness and failure	
E50ref	Secant stiffness in standard drained triaxial test	Ei x (2 – Rf) /2 (Ei = Initial stiffness)
Eoedref	Tangent stiffness for primary oedometer loading	E50ref
Eurref	Unload / reloading stiffness	3 x E50ref
m	Power for stress-level dependency of stiffness	0.5 ≤ m ≤ 1 (**0.5** for hard soil, 1 for soft soil)
C (C_{inc})	Effective cohesion (Increment of cohesion)	Failure parameter as in MC model
ϕ	Effective friction angle	Failure parameter as in MC model
ψ	Ultimate dilatancy angle	0 ≤ ψ ≤ ϕ
	Advanced parameters (Recommend to use Reference value)	
Rf	Failure Ratio (qf / qa)	0.9 (< 1)
Pref	Reference pressure	100
KNC	Ko for normal consolidation	1-sinϕ (< 1)
	Dilatancy cut-off	
Porosity	Initial void ratio	
Porosity(Max)	Maximum void ratio	Porosity < Porosity(Max)
	Cap yield surface	
OCR / Pc	Over Consolidation Ratio / Pre-overburden pressure	When entering both parameters, Pc has the priority of usage
α	Cap Shape Factor (scale factor of preconsolidation stress)	from KNC (Auto)
β	Cap Hardening Parameter	from Eoedref (Auto)

Fig. 9. Geotechnical Parameters to be used as input for MMC-Hardening soil model (Midas GTS NX Note Release, 2014).

Table 2. MMC-hardening parameter soil.

Depth (meter)	SPT Test	SPT Test	Soil type	e	n	E^{ref}_{50}	Eoed	Eur	C	ϕ (°)	ψ (°)	Ko
	N-SPT	N_{55}				(kg/m²)	(kg/m²)	(kg/m²)	(kg/m²)			
4	9	11	silty Sand	1.38	0.58	3.575	3.575	10.725	14.00	28.87	0.00	0.52
8	12	19	silty Sand	2.13	0.68	4.675	4.675	14.025	13.00	28.27	0.00	0.53
14	24	40	silty Sand	2.07	0.67	13.200	13.200	39.600	12.00	30.63	0.63	0.49
18	33	56	silty Sand	1.45	0.59	16.500	16.500	49.500	12.00	30.92	0.92	0.49
22	30	51	silty Sand	2.16	0.68	15.469	15.469	46.406	12.00	30.05	0.05	0.50
24	43	73	silty Sand	1.52	0.60	20.006	20.006	60.019	16.00	31.49	1.49	0.48

6. The Stage of Modelling, the Condition for Stability Analyses and Result of slope stability analysis

6.1 Stage of modelling analysis

The analysis of slope stability with cracked soil assumption was to be done through four stages, which are : Stage 1. To model the cracks inside the soil from interpretation of TR and IP mapping and value; Stage 2. To draw dimension and form of the slope; Stage 3. To establish the topographical data to become 3-dimension geometric picture; and Stage 4. To input the location of cracks at the 3D picture. All stages can be explained in **Fig. 10**.

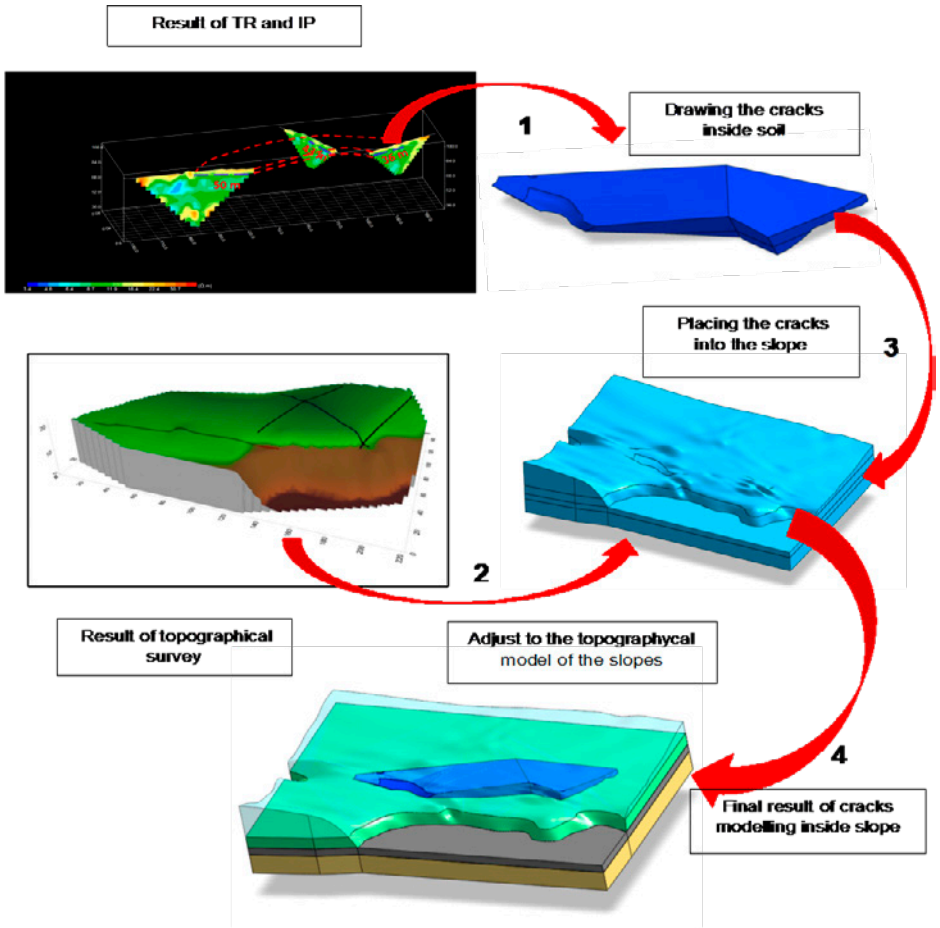

Fig. 10. Stages construction method before analysis with crack soil approach.

6.2 Result of analysis on maximum stresses and strain occuring inside slope

After landslide occurred at December 2nd, 2016, geoelectric measurement were conducted on the slide as well as boring on the soil with SPT. From those analysis and by means softwere Midas, the Safety Factor, SF = 1, was obtained and the maximum shear stress of 1.59 x 10^3 to 6.88 x 10^3 Kn/m^2 was estimated. The location of maximum strain of 2.5 that can be drawn as in **Fig. 11**. In **Fig. 11**, the highest concentration of stresses and strains should be given special attention, because these area can be predicted as the next location where sliding will be sliding

6.3 Validation of Latent Sliding in Research Location

The result of previous analysis showed the area highest concentration of stress and strain can be predicted to be next location to experience sliding. This has been proven in field that on January 16, 2017, another landslide did occurred and the new landslide was located exactly at the position showed by analysis using software. The location where the highest of stresses and strains was detected. The actual part of the remaining slope where failure occurred afterward as seen in **Fig. 12**.

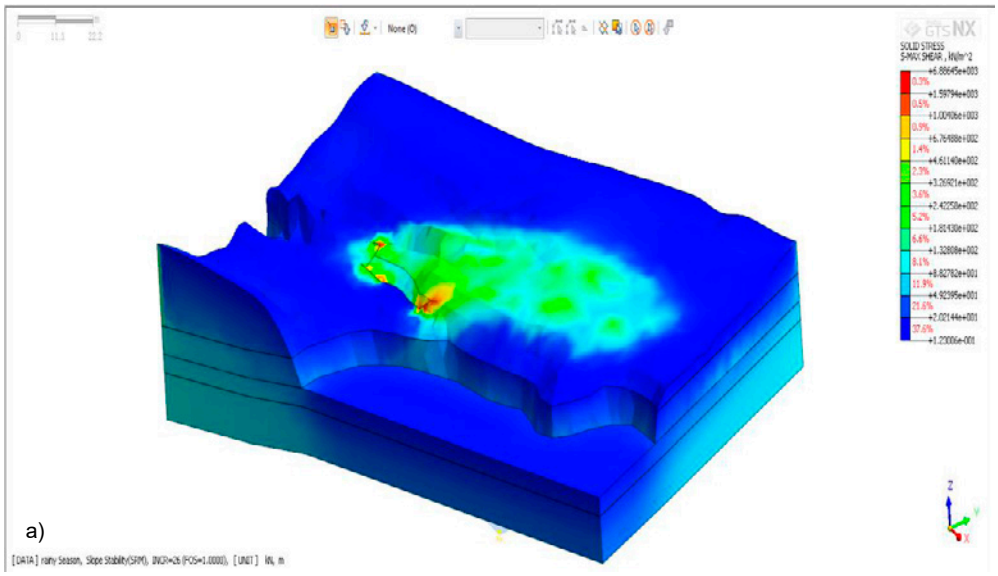

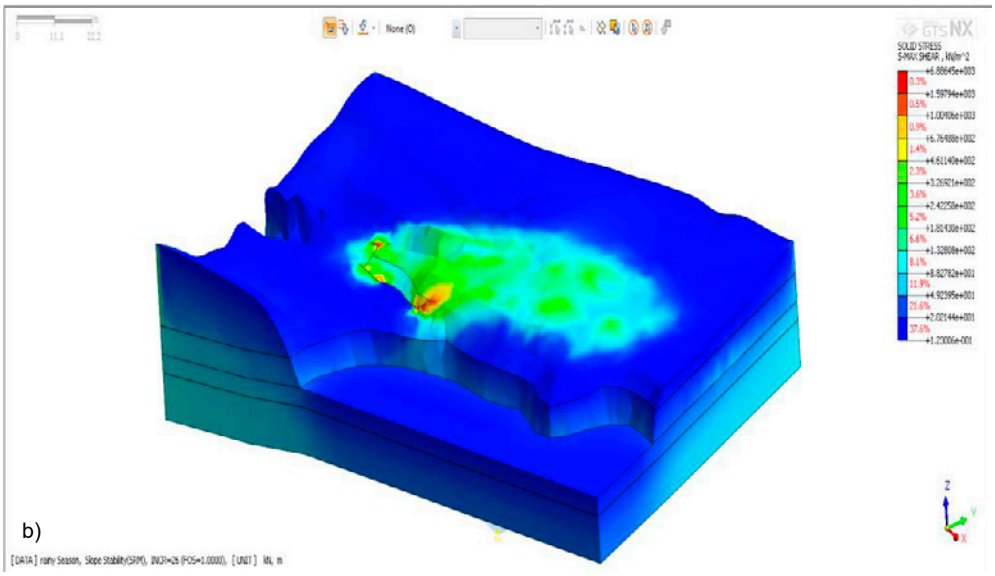

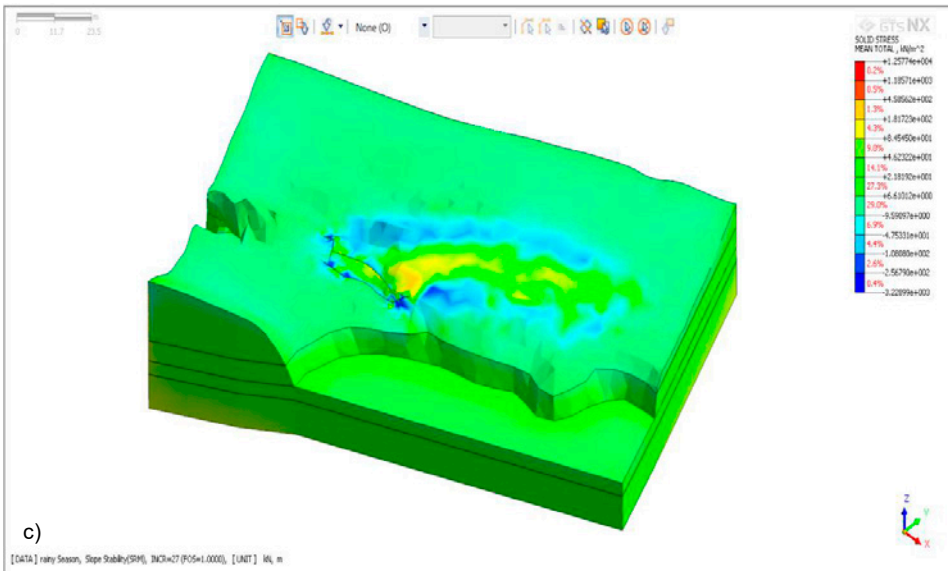

Fig. 11. The existence of area with maximum stresses and strain, inside the slope. (a). Result of analysis shows the concentration of maximum stresses are colored in red, (b). Result of analysis also shows the highest concentration of strain appeared in red color, (c). Result of analysis show mean total pressure.

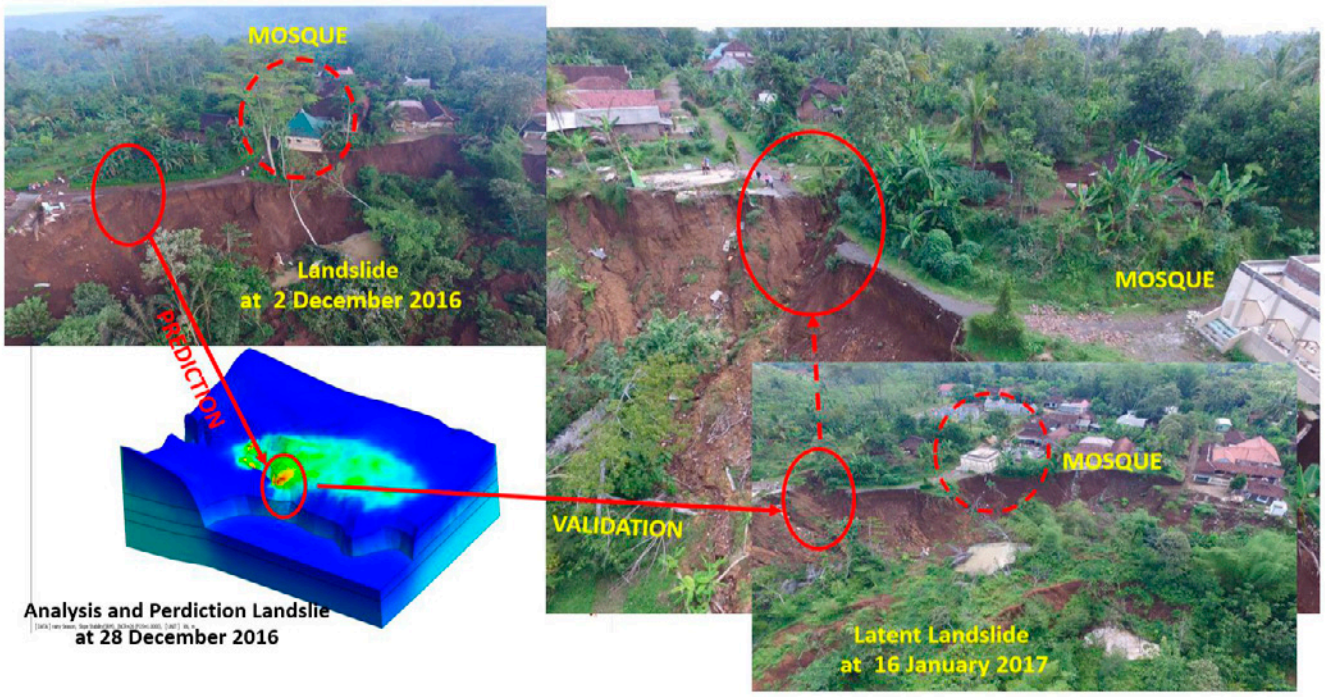

Fig. 12. The area where the highest stress and strain were found base on analysis of slope after failure in December 2016 and also the location where the next slide occurred in January 2017.

7. Conclusions

Based on this study, the following conclusions can be derived

1. The determination of location of cracks inside a slope is very important in assessment of slope future stability
2. The cracked soil approach has been successfully answered the problem of why slope sliding occurs and what the mechanism that causes the sliding
3. The analyses of slope sliding in the past were concentrated only in finding the Safety Factor, SF, of the slope which often gave unsatisfactory result. Many problems of slope sliding could still not be explained satisfactorily. This study has explained and shown how the mechanism in the slope to cause the slope to deform and lead to failure

Acknowledgements

This paper was supported by a Doctoral Program Grant from the Directorate General for Research and Development, Republic of Indonesia, 2017. The author wishes to express his gratitude for the support given to this work.

References

Stephanus, A., 2016. Identification of the existence and propagation of cracks inside soil slope through testing by tomographic resistivity and induced polarization method as a mean to explain the concept of cracked soils. P.hD Thesis, Civil Engr. Dept. of ITS, Institut Teknologi Sepuluh Nopember, Surabaya. (Unpublished).

Stephanus, A., Mochtar, I.B. and Widya, U., 2017. The measurement of water intrusion trough cracks propagation inside slope to explain the cause of slope failure – case study embankment in the sanggu buntok airport, central Kalimantan, Indonesia. Electronic Journal of Geotechnical Engineering: 5347 – 5362.

Duncan, J. M., 2000. Factor of safety and reliability in geotechnical engineering. Journal of Geotechnical and Geoenviromental Engineering: 307 – 316.

Fredlund, D.G. and Rahardjo, H., 1993. Soil mechanics for unsaturated soil. Jhon wiley and Sons Inc: pp 517.

Griffiths, D.V. and Lu, N., 2005. Unsaturated slope stability analysis with steady infiltration or evaporation using elasto-plastic finite element. International Journal Numerical Analysis Method Geomechanics, **29**: 249 – 267.

Security Monitoring, 2016) Focus on Extreme wheather

Mochtar, Indrasurya B, 2012. Field Evidences as the Basis for A Proposed New Concept of Soil Strength and Slope Stability, Proceeding, Annual Meeting of Indonesian Society of Geotechnical Engineering (PIT HATTI 2012), Jakarta.

Regmi, R.K., Nakagawa, H., Kawake, K., Yasuki, B. and Zhang, H., 2011. Experimental and numerical study of rainfall induced slope failure. Annual of Disas. Prev. Res. Inst.Kyoto Univ. No. 54 B.

Sánchez, M., Manzoli, O. L. and Guimarães, L. J. N., 2014. Modeling 3-D desiccation soil crack networks using a mesh fragmentation technique. Computers and Geotechnics, **62**: 27–39.

Tang, W.H., Stark, T.D. and Angulo, M., 1999. Reliability in back analysis of slope failures. Soils and Foundations, **39**(5): 73-80.

Wang, Y., Feng, D. and Ng, C. W. W., 2013. Modeling the 3D crack network and anisotropic permeability of saturated cracked soil. Computers and Geotechnics, **52**: 63-70.

Zhang, G., Wang, R., Qian, J., Zhang, J.M. and Qian, J., 2012. Effect study of cracks on behavior of soil slope under rainfall conditions. Soils and Foundations, **52**(4): 634-643.

Plaxis, 2012. Material Model Manual.

Rtomo and Rview Software. July 2016. Manual Geogiga Ver 6.1. Canada.

Symbols and abbreviations

E_U	Young Modulus
γ	Soil Density
E_{50}^{ref}	Stiffness Modulus At 50 % Strength at Certain Reference in Triaxial Test With Confining Pressure 100 KPa,
E_{oed}	Tangensial Modulus,
E_{ur}	Stiffness Modulus For Unloading and Reloading
c	Cohesion,
ϕ'	Angles of Internal Friction
ψ'	Angle of Dilatancy
N_{55}	Spt N Value Corrected To 55% Of The Theoretical Free Fall Hammer Energy